AIAA 82-4253

Minimum-Time Three-Dimensional Turn to a Point of Supersonic Aircraft

Ching-Fang Lin*
The University of Wisconsin-Madison, Madison, Wisconsin

The objective of this paper is to present real-time, on-line, minimum-time three-dimensional turn to a point of supersonic aircraft. The analytic aspect of the theory of optimal trajectories is emphasized. This includes the general properties of optimal trajectories consisting of the integrals of motion and the characteristic features in engine and aerodynamic controls. By using the integrals of motion the totality of the optimal trajectories can be obtained as a family of curves depending on a certain number of arbitrary constants. The optimal control is obtained by geometrical method through the domain of maneuverability. This makes explicit the switching characteristics of the optimal control, in particular when singular or chattering control is involved. The optimality of singular thrust control and the optimal junction of different subarcs are analyzed. The computation of the optimal trajectories is carried out using the aerodynamic and engine characteristics of a lightweight, high thrust-to-weight ratio supersonic fighter. By using normalized control variables, i.e., the thrust-to-weight ratio, the bank angle, and the load factor, results can be applied to any supersonic aircraft.

Nomenclature

a = speed of sound = $a(Z)$ given as a tabular function; dimensionless aerodynamic force = A/W
A = aerodynamic force
C_D = drag coefficient = $C_{D_0}(M) + K(M)C_L^2$
C_{D_0} = zero-lift drag coefficient = $C_{D_0}(M)$
C_i = constants of integration, where $i = 0,1,\ldots$
C_L = lift coefficient
C_L^* = lift coefficient corresponding to $E^*(M) = C_L^*(M) = \sqrt{C_{D_0}(M)/K(M)}$
$C_{L_{max}}$ = maximum lift coefficient = $C_{L_{max}}(M)$
d = dimensionless drag force = $D/W = 1/2E^*[\Delta + (l^2/\Delta)]$ referred to as the parabolic drag polar
D = drag force = $\frac{1}{2}\rho(Z)V^2SC_D$
E^* = maximum lift-to-drag ratio = $E^*(M) = 1/2\sqrt{K(M)C_{D_0}(M)}$
g = acceleration of the gravity = const
H = Hamiltonian
H^* = maximized Hamiltonian
$\bar{H}$ = reduced Hamiltonian = $\boldsymbol{P}\cdot\boldsymbol{a}$
$\bar{H}^*$ = maximized reduced Hamiltonian
k = ratio of specific heats = 1.4
K = induced drag factor
l = dimensionless lift force = $n = L/W$
L = lift force = $\frac{1}{2}\rho(Z)V^2SC_L$
M = Mach number = $V/a(Z)$
n = load factor = $l = L/W = M^2C_L/\omega$
n_s = physiological/structural constraint on n
p = ambient pressure = $p(Z)$ given as a tabular function
$\boldsymbol{P}$ = see $\bar{H}$
P_s = adjoint variable associated with state variable s
q = dynamic pressure = $\rho(Z)V^2/2 = kp(Z)M^2/2$
S = wing area of aircraft
t = time
T = thrust magnitude = $\zeta T_{max}(M,Z)$
T_{max} = maximum thrust = $T_{max}(M,Z)$
V = velocity
$\boldsymbol{V}$ = velocity vector
W = weight of aircraft
x,y,z = Cartesian coordinates
X,Y,Z = Cartesian coordinates
X = longitudinal range
Y = lateral range
Z = altitude
α = angle of attack
γ = flight path angle
Δ = defined as $M^2C_L^*(M)/\omega$
ζ = thrust control parameter = $T/T_{max}(M,Z)$
ρ = atmospheric density = $\rho(Z)$ given as a tabular function
τ = thrust-to-weight ratio = T/W
τ_{max} = maximum thrust-to-weight ratio = $\tau_{max}(M,\omega) = T_{max}/W$
ϕ = bank angle
ψ = heading
ω = dimensionless wing loading = $2W/kp(Z)S$

Subscripts

c = chattering condition
f = final value
max = maximum value
min = minimum value
M = logarithmic derivative as in $F_M = d\log F/d\log M = M/F(dF/dM)$
0 = initial value

Received March 31, 1981; revision received March 15, 1982.

*Assistant Professor, Department of Electrical and Computer Engineering. Member AIAA.

Introduction

THE advancement of present-day aerospace technology has led to the production of a new generation of fighter aircraft. The development requirements of these aircraft have motivated a considerable effort to analyze their optimum maneuvers at very high speed.[1] In optimum maneuvers of supersonic aircraft in three dimensions, a straightforward application of the maximum principle always leads to a two-point boundary-value problem involving several arbitrary parameters. Furthermore, the complexity of the problem increases with the combination of three control variables, i.e., τ, ϕ, and n, which are subject to various constraints. Hence, the optimization problems solved thus far generally have been reduced-order problems with constraints on the state so that the flight is either on a horizontal plane[2-4] or on a vertical

plane.[5-9] In the analysis of three-dimensional supersonic aircraft maneuvers, simplified approximate solution can be obtained from a reduced-order model based on energy-state approximation.[10-12] In general, for any specified aircraft characteristics, when direct numerical optimization technique is applied, the structure of the optimal control, in terms of the thrust and aerodynamic modulation, is not characteristically displayed and the general behavior of the optimal trajectory is not clearly understood except for the specific example considered. Results obtained from this kind of pure numerical technique are restricted to a particular set of terminal conditions for a specified aircraft model. In this paper the maximum principle is used to analyze three-dimensional turning performance of a typical lightweight, high thrust-to-weight ratio supersonic fighter.[1] The aerodynamic and engine characteristics are modeled as continuous functions of state variables. In addition, several techniques are used to alleviate the difficulties encountered in the problem.

Equations of Motion

If the thrust is considered as nearly aligned with V, the motion of a point mass lifting vehicle over a flat nonrotating Earth, with the assumption of symmetrical flight, is governed by the following set of nonlinear ordinary differential equations.[1]

$$\dot{X}=V\cos\gamma\cos\psi \qquad \dot{V}=g\left(\frac{T-D}{W}-\sin\gamma\right)$$

$$\dot{Y}=V\cos\gamma\sin\psi \qquad \dot{\gamma}=\frac{g}{V}\left(\frac{L\cos\phi}{W}-\cos\gamma\right)$$

$$\dot{Z}=V\sin\gamma \qquad \dot{\psi}=\frac{g}{V}\frac{L}{W}\frac{\sin\phi}{\cos\gamma} \tag{1}$$

The duration of the three-dimensional turning flight is relatively short so the weight is considered practically constant. In Eq. (1) the aerodynamic force A is decomposed into a drag force D opposite to V and a lift force L perpendicular to V; the thrust is always on the lift-drag plane. We evaluate the aerodynamic force using a rotating coordinate system $Mxyz$ with the origin M at the center of the mass of the aircraft, the x axis along V, the z axis along the lift force, and the y axis completing a right-handed system (Fig. 1). To fix the orientation of the rotating axes, the local horizontal system $MX_hY_hZ_h$ is used. It is defined as the system with the origin M having its axes always parallel to the Earth-fixed reference system $OXYZ$. To go from the $MX_hY_hZ_h$ system to the $Mxyz$ system it is necessary to pass through two intermediate systems, $Mx_1y_1z_1$ and $Mx_2y_2z_2$. The former is obtained from the $MX_hY_hZ_h$ system by rotating ψ about the Z_h axis; the latter is obtained from the $Mx_1y_1z_1$ system by rotating γ about the y_1 axis. The $Mxyz$ system is then obtained from the $Mx_2y_2z_2$ system by rotating ϕ about the x_2 axis. By controlling the ailerons, the rotation of L about V creates a lateral component of L. This is assuming that L is rotated by means of ϕ out of the vertical plane containing V. Hence, ϕ is the orientation of A with respect to this plane; it is the angle formed by L and this plane. The vector L is thus decomposed into $L\cos\phi$ which lies on the vertical plane and is perpendicular to V, and $L\sin\phi$ which is perpendicular to the vertical plane. As seen in Fig. 1, V, $L\sin\phi$, and $L\cos\phi$, respectively, lie along the x_2 axis, y_2 axis, and z_2 axis of the $Mx_2y_2z_2$ system. Hence, it is appropriate to decompose A along these axes so that

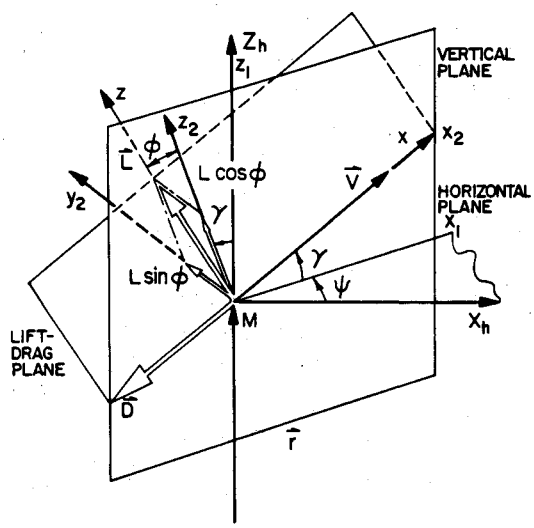

Fig. 1 Aerodynamic forces.

$$A=-Di_2+L\sin\phi j_2+L\cos\phi k_2 \tag{2}$$

where (i_2, j_2, k_2) is the set of unit vectors associated with the $Mx_2y_2z_2$ system. In the $Mx_2y_2z_2$ system the dimensionless lift force l and the dimensionless drag force d are, respectively,

$$l=l\sin\phi j_2+l\cos\phi k_2 \tag{3}$$

and

$$d=-di_2 \tag{4}$$

Using Eq. (2), a is

$$a=(-di_2+l\sin\phi j_2+l\cos\phi k_2)=d+l \tag{5}$$

Because of the lift-drag relation, the flight is controlled by C_L (which is equivalent to α), ϕ, and T.

Optimal Control

The Hamiltonian to the variation problem is

$$H=P_X V\cos\gamma\cos\psi+P_Y V\cos\gamma\sin\psi+P_Z V\sin\gamma$$
$$+P_V g\left(\frac{T-D}{W}-\sin\gamma\right)$$
$$+P_\gamma\frac{g}{V}\left(\frac{L\cos\phi}{W}-\cos\gamma\right)+P_\psi\frac{g}{V}\frac{L}{W}\frac{\sin\phi}{\cos\gamma} \tag{6}$$

where P_s fulfills the adjoint equation

$$\frac{dP_s}{dt}=-\frac{\partial H^*}{\partial s} \tag{7}$$

where H^* is the maximized Hamiltonian. Since X and Y coordinates are ignorable, the following integrals can be obtained.

$$P_X=C_1, \qquad P_Y=C_2 \tag{8}$$

In addition,

$$\frac{dP_\psi}{dt}=P_X V\cos\gamma\sin\psi-P_Y V\cos\gamma\cos\psi=\frac{d}{dt}(C_1Y-C_2X) \tag{9}$$

produces another integral

$$P_\psi=C_1Y-C_2X+C_3 \tag{10}$$

The fact that H is independent of t produces the fourth integral

$$H=C_0 \tag{11}$$

The problems considered here are minimum-time problems. Hence, to maximize H, $C_0>0$ has to be true. By using the Hamiltonian integral only two of the three remaining adjoint variables P_Z, P_V, and P_γ need to be found. In vertical flight all three variables are involved, causing difficulty in solving the optimization problem. This difficulty is also present in three-dimensional flight problems. As compared to vertical flight, three-dimensional flight has two more variables, i.e., Y and ψ, that may pose a problem in obtaining the optimal solution. However, P_Y and P_ψ, associated with Y and ψ, have been found in Eqs. (8) and (10), respectively. In horizontal flight P_Z and P_γ are not present, and the remaining P_V is given by the Hamiltonian integral. The problem is completely solved by Lin in Ref. 1.

The load factor n is used as a lift control variable to represent α. Because of physiological/structural constraint, n is bounded by an upper value n_s. On the other hand, C_L is bounded by an upper value $C_{L_{\max}}(M)$ which is a function of the Mach number. Hence, the bounds on n are

$$|n| \le n_{\max} = \min.\left[n_s, \frac{M^2 C_{L_{\max}}(M)}{\omega}\right] \tag{12}$$

where $n_{\max}$ is the maximum permissible load factor for either $C_L = C_{L_{\max}}$ or $n = n_s$. Constraint Eq. (12) on n assumes that ϕ is unconstrained. However, if ϕ is subject to the constraint

$$|\phi| \le \phi_{\max} \tag{13}$$

where $\phi_{\max}$ can either be a constant or a function of the state variable depending on the problem considered, then constraint Eq. (12) on n becomes

$$n_{\min} \le n \le n_{\max} \tag{14}$$

where $n_{\min}$ is the lower bound of n which corresponds to $C_{L_{\min}}$, i.e., the lower bound of the lift coefficient. The domain of flight[1] may be further restricted by the line of maximum dynamic pressure

$$M^2 \le \frac{2q_{\max}}{kp} = \frac{S}{W}\omega q_{\max} \tag{15}$$

and the line of maximum Mach number obtained by solving the equation $dV/dt = 0$ *with* $\tau = \tau_{\max}$ so that

$$\tau_{\max} = d + \sin\gamma \tag{16}$$

Hamiltonian Eq. (6) is rewritten as

$$H = C_1 V\cos\gamma\cos\psi + C_2 V\cos\gamma\sin\psi + P_Z V\sin\gamma$$
$$+ P_V g\left[\zeta\tau_{\max}(M,\omega) - \frac{l}{2E^*}\left(\Delta + \frac{n^2}{\Delta}\right) - \sin\gamma\right]$$
$$+ P_\gamma \frac{g}{V}(n\cos\phi - \cos\gamma) + P_\psi \frac{gn\sin\phi}{V\cos\gamma} \tag{17}$$

In this formulation, the control variables are ζ, ϕ, and n where ζ is subject to the constraint $0 \le \zeta \le 1$. For unbounded ϕ, n is subject to constraint Eq. (12). However, for bounded ϕ, n is subject to constraint Eq. (14). It is assumed that $C_{D_0}(M)$, $K(M)$, and $C_{L_{\max}}(M)$ are known functions of the Mach number, and that $\tau_{\max}(M,\omega)$ is a function of both the Mach number and ω. For numerical computation, we use the data of a supersonic fighter assembled by Lin,[1] but the same procedure can be applied to any other set of data.

Optimal Thrust Control

For the thrust control, we consider P_V, called the switching function. To maximize H, if

$P_V > 0$,	$\xi = 1$	boost arc	
$P_V < 0$,	$\zeta = 0$	coast arc	(18)
$P_V \equiv 0$	$\zeta =$ variable	sustained arc	

for $t \in [t_1, t_2]$

The last case of sustained arc is the singular thrust arc along which the thrust is at an intermediate level. The optimal trajectory is a combination of boost arc (B arc), coast arc (C arc), and sustained arc (S arc).

Optimal Aerodynamic Control

The aerodynamic control consists of ϕ and n, i.e., l. Figure 2 shows the domain of maneuverability described by the terminus of $\boldsymbol{a}$. This domain of maneuverability is a surface of revolution Σ about the x_2 axis. It is bounded by constraint Eq. (12) in the case where ϕ is unbounded; it is bounded by constraint Eqs. (13) and (14) in the case where ϕ is bounded. The domain of maneuverability is a parabolic drag polar on the plane formed by the x axis and the z axis. In order to obtain the optimal aerodynamic control, H is expressed in another form as

$$H = g\left[-\frac{P_V}{2E^*}\left(\Delta + \frac{l^2}{\Delta}\right) + \frac{P_\psi}{V\cos\gamma} l\sin\phi + \frac{P_\gamma}{V} l\cos\phi\right] + \ldots \tag{19}$$

where the remaining terms are independent of l and ϕ.

In obtaining the optimal aerodynamic control, it is sufficient to reduce H to that which contains only l and ϕ. By using the parabolic drag polar the reduced Hamiltonian is then

$$\tilde{H} = -P_V d + \frac{P_\psi}{V\cos\gamma} l\sin\phi + \frac{P_\gamma}{V} l\cos\phi \tag{20}$$

This reduced Hamiltonian can be regarded as

$$\tilde{H} = \boldsymbol{P}\cdot\boldsymbol{a} \tag{21}$$

with

$$\boldsymbol{P} = P_1 \boldsymbol{i}_2 + P_2 \boldsymbol{j}_2 + P_3 \boldsymbol{k}_2 \tag{22}$$

where

$$P_1 = P_V, \qquad P_2 = P_\psi / V\cos\gamma, \qquad P_3 = P_\gamma / V \tag{23}$$

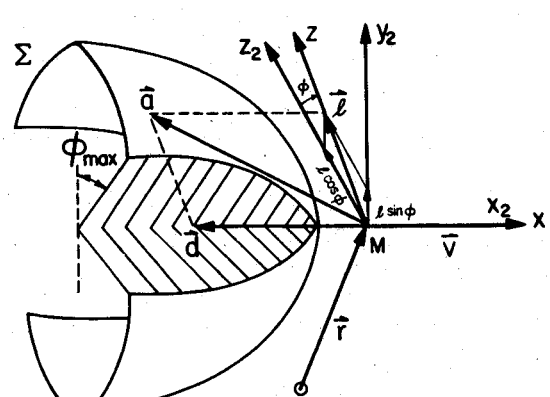

Fig. 2 Domain of maneuverability for the aerodynamic force.

To obtain the optimal aerodynamic control, $\boldsymbol{a}$ has to be chosen so that at every instant $\bar{H}$ reaches its maximum. In the domain of maneuverability, this optimal condition leads to the selection of the optimal $\boldsymbol{a}$ such that the projection of $\boldsymbol{a}$ on $\boldsymbol{P}$ is maximized. For this, the four different arcs of the aerodynamic control are 1) interior bank angle and interior load factor, 2) interior bank angle and boundary load factor, 3) boundary bank angle and interior load factor, and 4) boundary bank angle and boundary load factor.

For the first two arcs where ϕ is unbounded, the aeodynamic control law requires that $\boldsymbol{a}$, whose terminal point touches a plane which is tangent to Σ and concurrently perpendicular to $\boldsymbol{P}$, be obtained (Fig. 3). In order to satisfy this optimal condition, the following procedure is considered. First, a plane which is tangent to Σ and contains a point in contact with the terminus of $\boldsymbol{a}$ is always perpendicular to the lift-drag plane. Therefore, in order for this plane to be perpendicular to $\boldsymbol{P}$ to satisfy the preceding optimal condition, the lift-drag plane must contain $\boldsymbol{P}$. This can be achieved by rotating the lift-drag plane away from the vertical plane about $\boldsymbol{V}$ by a certain angle ϕ as shown in Fig. 3. This causes $\boldsymbol{l}$ to lie on the projection of $\boldsymbol{P}$ on the plane formed by the y_2 axis and z_2 axis, as represented by Λ in the figure, where

$$\Lambda=\epsilon\sqrt{P_2^2+P_3^2}; \qquad \epsilon=\pm 1 \tag{24}$$

Hence, the above optimal interior ϕ can be obtained by

$$l\sin\phi/l\cos\phi=P_2/P_3, \quad \text{i.e., } \tan\phi=P_\psi/P_\gamma\cos\gamma \tag{25}$$

which is equivalent to the maximum of $\Lambda\cdot l$.

Under this optimal condition $\boldsymbol{P}$ is expressed as

$$\boldsymbol{P}=P_l\boldsymbol{i}+\Lambda\boldsymbol{k} \tag{26}$$

that is, it is on the lift-drag plane as shown in Fig. 4a, where

$$\boldsymbol{a}=-d\boldsymbol{i}+l\boldsymbol{k} \tag{27}$$

The set of vectors $(\boldsymbol{i}, \boldsymbol{j}, \boldsymbol{k})$ in Eqs. (26) and (27) represents the unit vectors associated with the $Mxyz$ system. As seen in Fig. 4a, when l varies within constraint Eq. (12), $\boldsymbol{a}=(-d,l)$ describes the domain of maneuverability which is the parabolic drag polar. To maximize $\bar{H}$, l has to be selected so that at the terminus of $\boldsymbol{a}$ the tangent to the parabolic drag polar is perpendicular to $\boldsymbol{P}$. This results in an angle β formed between this tangent and the z axis having the same value as the angle β formed between $\boldsymbol{P}$ and the x axis. Hence,

$$\tan\beta=\frac{\partial d}{\partial l}, \quad \text{i.e.,} \quad \frac{\Lambda}{P_l}=\frac{l}{\Delta E^*} \tag{28}$$

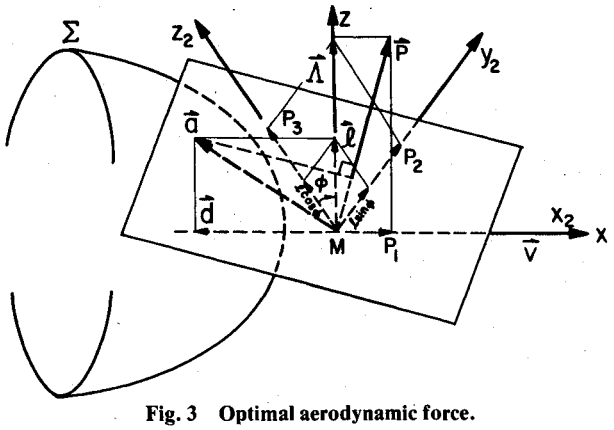

Fig. 3 Optimal aerodynamic force.

leads to

$$n^2=\frac{\Delta^2E^{*2}}{V^2P_V^2}\left(P_\gamma^2+\frac{P_\psi^2}{\cos^2\gamma}\right) \tag{29}$$

By applying Eq. (25) to the preceding equation, we have

$$n=\Delta E^*P_\gamma/VP_V\cos\phi \tag{30}$$

If $\boldsymbol{P}$, with components P_l and Λ, is inside the angle $\Delta_1M\Delta_2$, then the optimal load factor used is an interior load factor as given in Eq. (30). As seen in Fig. 4a, a necessary condition for interior n is that $P_l>0$, i.e., $P_V>0$. From condition Eq. (18) interior n is used with B arc. In addition, for positive interior n it is necessary that $\epsilon=1$; for negative interior n, it is necessary that $\epsilon=-1$. If $\boldsymbol{P}$ is outside the angle $\Delta_1M\Delta_2$, then the optimal load factor used is boundary load factor, either $n=-n_{\max}$ or $n=n_{\max}$, depending on whether $\bar{H}_1^*>\bar{H}_2^*$ or $\bar{H}_2^*>\bar{H}_1^*$, where

$$\bar{H}_1^*=\boldsymbol{P}\cdot\boldsymbol{a}_1, \qquad \bar{H}_2^*=\boldsymbol{P}\cdot\boldsymbol{a}_2 \tag{31}$$

with

$$\boldsymbol{a}_1=(-d,-n_{\max}), \qquad \boldsymbol{a}_2=(-d,n_{\max}) \tag{32}$$

If $\epsilon>0$, then $\bar{H}_2^*>\bar{H}_1^*$, hence $n=n_{\max}$. If $\epsilon<0$, then $\bar{H}_1^*>\bar{H}_2^*$, hence $n=-n_{\max}$. It is clear that when $P_l\le 0$, i.e., when $P_V\le 0$, boundary n is used. This, of course, is on a C or S arc. On the other hand, a B arc can be flown with either an interior or a boundary n. In the case $\boldsymbol{P}=\boldsymbol{P}_c$ where $\bar{H}_1^*=\bar{H}_2^*$ for a finite time interval, i.e., when $P_V<0$ and $\Lambda\equiv 0$ for a finite time interval, there may exist a chattering control with C arc in which n rapidly switches between $-n_{\max}$ and $n_{\max}$ in order to maximize the deceleration. In the case where $P_V>0$ and $\Lambda\equiv 0$ for a finite time interval, there may exist a period of flight with B arc and $n=0$.

For the third and the fourth arcs where ϕ is bounded, whenever ϕ as computed by Eq. (25) exceeds $\phi_{\max}$, the optimal bank angle is on the boundary $\phi=\phi_{\max}$. Otherwise,

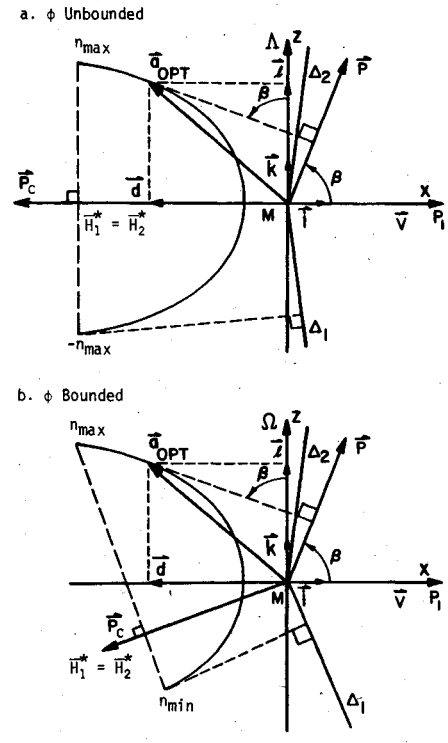

Fig. 4 Domain of maneuverability for the load factor: a) ϕ unbounded and b) ϕ bounded.

interior ϕ is used and n is either in the interior or on the boundary as described previously. When $\phi=\phi_{\max}$, P in the reduced Hamiltonian Eq. (21) becomes

$$P=P_l i+\Omega_l k \tag{33}$$

where

$$\Omega=P_\gamma\cos\phi_{\max}/V+P_\psi\sin\phi_{\max}/V\cos\gamma \tag{34}$$

that is, it is also on the lift-drag plane as shown in Fig. 4b. As in the first two arcs where ϕ is unbounded, when l varies within constraint Eq. (14), $a=(-d, l)$ describes the domain of maneuverability (Fig. 4b) which is the parabolic drag polar. To maximize $\bar{H}$, l must be selected so that at the terminus of a the tangent to the parabolic drag polar is perpendicular to P. This results in an angle β formed between this tangent and the z axis having the same value as the angle β formed between P and the x axis. Hence,

$$\tan\beta=\frac{\partial d}{\partial l}, \quad \text{i.e.,} \quad \frac{\Omega}{P_l}=\frac{l}{\Delta E^*} \tag{35}$$

leads to

$$n=\frac{\Delta E^*}{VP_V}\left(P_\gamma\cos\phi_{\max}+\frac{P_\psi\sin\phi_{\max}}{\cos\gamma}\right) \tag{36}$$

If P, with components P_l and Ω, is inside the angle $\Delta_l M\Delta_2$, then the optimal load factor used is an interior load factor as given in Eq. (36). As seen in Fig. 4b, a necessary condition for interior n is that $P_l>0$, i.e., $P_V>0$. From condition Eq. (18), interior n is used with B arc. If P is outside the angle $\Delta_l M\Delta_2$, then the optimal load factor used is boundary load factor, either $n=n_{\min}$ or $n=n_{\max}$ depending on whether $\bar{H}_1^*>\bar{H}_2^*$ or $\bar{H}_2^*>\bar{H}_1^*$, where $\bar{H}_1^*$ and $\bar{H}_2^*$ are defined in Eqs. (31), and a_2 is the same as that in Eq. (32). However, now

$$a_l=(-d, n_{\min}) \tag{37}$$

From Fig. 4b, if P is above P_c, then $\bar{H}_2^*>\bar{H}_1^*$, hence $n=n_{\max}$. If P is below P_c, then $\bar{H}_2^*<\bar{H}_1^*$, hence $n=n_{\min}$. It is clear that when $P_l\le 0$, i.e., when $P_V\le 0$, boundary n is used. This, of course, is on a C or S arc. On the other hand, a B arc can be flown with either an interior or a boundary n. In the case $P=P_c$ where $\bar{H}_1^*=\bar{H}_2^*$ for a finite time interval, there may exist a chattering control with C arc in which n rapidly switches between $n_{\min}$ and $n_{\max}$. As $n_{\min}$ becomes larger, $M\Delta_l$ moves upward and P_c moves downward, until $n_{\max}=n_{\min}$; then $M\Delta_l=M\Delta_2$ and $P_c=-|P_c|k$. In the case where $P_V>0$ and $\Omega\equiv 0$ for a finite time interval, there may exist a period of flight with B arc and $n=0$ as long as $n_{\min}\le 0$.

From the previously given four arcs of the aerodynamic control, it is seen that the optimal aerodynamic controls are functions of P_V, $P\gamma$, and P_ψ associated with V. Since P_ψ is known, the adjoint variables remaining to be found are P_V and P_γ. Their differential equations are coupled with the equation of P_Z. With the existing integrals one of the three adjoint equations of P_V, P_γ, and P_Z can be deleted. It is found that in order to save substantial computation time and to enhance real-time, on-line optimization, it is simpler to integrate the adjoint equations of P_V and P_γ and obtain P_Z from the existing integrals. From Hamiltonian Eq. (17) we deduce the adjoint equations of P_V and P_γ. For interior ϕ and interior n,

$$\frac{\mathrm{d}VP_V}{\mathrm{d}t}=-C_0+P_V g\left\{\zeta\tau_{\max}(2-\tau_{\max_M})-2\sin\gamma+\frac{1}{2E^*}\left[\left(\Delta-\frac{n^2}{\Delta}\right)C_{L_M}^*-\left(\Delta+\frac{n^2}{\Delta}\right)E_M^*-\frac{4n^2}{\Delta}\right]\right\}+P_\gamma\frac{2g}{V}(n\cos\phi-\cos\gamma)+P_\psi\frac{2gn\sin\phi}{V\cos\gamma}$$

$$\frac{\mathrm{d}P_\gamma}{\mathrm{d}t}=C_l V\sin\gamma\cos\psi+C_2 V\sin\gamma\sin\psi-P_Z V\cos\gamma+P_V g\cos\gamma-P_\gamma\frac{g\sin\gamma}{V}-P_\psi\frac{gn\sin\phi\sin\gamma}{V\cos^2\gamma} \tag{38}$$

In the preceding equations the Hamiltonian integral has been used for simplification. In Eqs. (38), $\zeta=1$, ϕ is given in Eq. (25) and n is given in Eq. (30). For interior ϕ and boundary n, if $n=n_s$, then the adjoint equations are given in Eqs. (38) with ϕ given in Eq. (25). If $n=M^2C_{L_{\max}}/\omega$, then

$$\frac{\mathrm{d}VP_V}{\mathrm{d}t}=-C_0+P_V g\left\{\zeta\tau_{\max}(2-\tau_{\max_M})-2\sin\gamma+\frac{1}{2E^*}\left[\left(\Delta-\frac{n^2}{\Delta}\right)C_{L_M}^*-\left(\Delta+\frac{n^2}{\Delta}\right)E_M^*+\frac{2n^2}{\Delta}C_{L_{\max_M}}\right]-P_\gamma\frac{g}{V}\left(2\cos\gamma+n\cos\phi C_{L_{\max_M}}\right)-P_\psi\frac{gn\sin\phi}{V\cos\gamma}C_{L_{\max_M}}$$

$$\frac{\mathrm{d}P_\gamma}{\mathrm{d}t}=C_l V\sin\gamma\cos\psi+C_2 V\sin\gamma\sin\psi-P_Z V\cos\gamma+P_V g\cos\gamma-P_\gamma\frac{g\sin\gamma}{V}-P_\psi\frac{gn\sin\phi\sin\gamma}{V\cos^2\gamma} \tag{39}$$

In the preceding equations, ϕ is given in Eq. (25). For boundary ϕ and interior n, if $\phi_{\max}$ is a constant, then the adjoint equations are given in Eqs. (38) with $\zeta=1$, $\phi=\phi_{\max}$ and n is given in Eq. (36). For boundary ϕ and boundary n, if $n=n_s$, then for a constant $\phi_{\max}$ the adjoint equations are given in Eqs. (38) with $\phi=\phi_{\max}$. If $n=M^2C_{L_{\max}}/\omega$, then for a constant $\phi_{\max}$ the adjoint equations are given in Eqs. (39) with $\phi=\phi_{\max}$. If $n=n_{\min}$, then for a constant $\phi_{\max}$ and a constant $n_{\min}$ the adjoint equations are given in Eqs. (38) with $\phi=\phi_{\max}$.

Optimal Switching

The behavior of the switching function P_V determines the thrust magnitude control. At the junction of the different thrust control arcs, the switching function P_V is zero. It suffices to analyze the sign of $\mathrm{d}P_V/\mathrm{d}t$ at $P_V=0$ to determine the optimal switching. For a junction between two nonsingular thrust arcs, a C-B sequence is optimum if at the junction $\mathrm{d}P_V/\mathrm{d}t>0$. For a reverse condition, a B-C sequence is optimum. In the case where $\mathrm{d}P_V/\mathrm{d}t=0$ at the switching point, the optimal switching is determined upon analyzing the high-order derivative of the switching function.[13]

As seen in Fig. 4, if $P\neq 0$ at the switching point, then boundary n is used. With n on the boundary and $P_V=0$, by using the Hamiltonian integral we have

$$\frac{\mathrm{d}P_V}{\mathrm{d}t}=-\frac{\partial H^*}{\partial V}=\frac{1}{V}\left\{-C_0+P_\gamma\left[\frac{2g}{V}(n\cos\phi-\cos\gamma)-g\cos\phi\frac{\partial n}{\partial V}\right]+P_\psi\left(\frac{2gn\sin\phi}{V\cos\gamma}-\frac{g\sin\phi}{\cos\gamma}\frac{\partial n}{\partial V}\right)\right\} \tag{40}$$

If $n=n_s$ at the switching point, then $\partial n/\partial V=0$ and Eq. (40) becomes

$$\frac{dP_V}{dt}=\frac{1}{V}\left[-C_0+P_\gamma\frac{2g}{V}(n_s\cos\phi-\cos\gamma)+P_\psi\frac{2gn_s\sin\phi}{V\cos\gamma}\right] \quad (41)$$

Using this equation, a switching from a C arc to a B arc is optimum if

$$P_\gamma\frac{2g}{V}(n_s\cos\phi-\cos\gamma)+P_\psi\frac{2gn_s\sin\phi}{V\cos\gamma}>C_0 \quad (42)$$

For a switching from a B arc to a C arc to be optimum, the preceding inequality is reversed. Along an S arc, which is a singular thrust arc, $P_V\equiv 0$ for a finite time interval. Hence, we constantly have $dP_V/dt=0$. By taking the derivative of this equation, where dP_V/dt is given in Eq. (41), we have an equation for the linear thrust control

$$\frac{d^2P_V}{dt^2}=-\frac{C_0g}{V^2}\zeta\tau_{\max}+(\ldots)=0 \quad (43)$$

Since the order of the singular thrust arc is $q=1$, according to the generalized Legendre-Clebsch condition, for optimal condition the coefficient of $\zeta\tau_{\max}$ must be non-negative. However, since we know that $C_0>0$, the optimal condition is not satisfied.

If $n=M^2C_{L_{\max}}(M)/\omega$ at the switching point, then Eq. (40) becomes

$$\frac{dP_V}{dt}=-\frac{1}{V}\left[C_0+P_\gamma\frac{g}{V}(2\cos\gamma+n\cos\phi C_{L_{\max_M}})+P_\psi\frac{gn\sin\phi}{V\cos\gamma}C_{L_{\max_M}}\right] \quad (44)$$

Using this equation, a switching from a C arc to a B arc is optimum if

$$C_0+P_\gamma\frac{g}{V}(2\cos\gamma+n\cos\phi C_{L_{\max_M}})+P_\psi\frac{gn\sin\phi}{V\cos\gamma}C_{L_{\max_M}}<0 \quad (45)$$

This inequality is reverse for a switching from a B arc to a C arc to be optimum. Along an S $dP_V/dt=0$ for a finite time interval. By taking the derivative of arc, we have $P_V=0$ and $dP_V/dt=0$, where dP_V/dt is given in Eq. (44), we have the equation for the linear thrust control

$$d^2P_V/dt^2=A\zeta\tau_{\max}+(\ldots)=0 \quad (46)$$

where the coefficient of $\zeta\tau_{\max}$ has the form

$$A=-\frac{g}{V^2}\left\{C_0+C_{L_{\max_M}}\left(P_\gamma\frac{gn\cos\phi}{V}+P_\psi\frac{gn\sin\phi}{V\cos\gamma}\right)\left[2+C_{L_{\max_M}}+\left(C_{L_{\max_M}}\right)_M\right]\right\} \quad (47)$$

with non-negative A for the optimal condition. Obviously, this optimal condition is not satisfied with $C_{L_{\max}}$ independent of the Mach number. This is particularly true in the case of maneuver at low Mach number. For any prescribed function $C_{L_{\max}}(M)$, the explicit condition $A\geq 0$ defines a small region in the state variable and adjoint variable space where S arc can be optimal.

In the case where $P=0$ and the interior ϕ is used at the switching point, from Eq. (26) we have $\Lambda=0$. Hence, $P_2=0$ and $P_3=0$ which implies that $P_\gamma=0$ and $P_\psi=0$ as long as $V\cos\gamma\neq 0$. From Eq. (25) and Eq. (30), the limiting values of ϕ and n at this point are, respectively,

$$\tan\phi=a_1/a_2 \quad (48)$$

and

$$n=\Delta E^*a_2/C_0\cos\phi\sin\gamma \quad (49)$$

where

$$a_1=V\sin\gamma(C_2\cos\psi-C_1\sin\psi)$$
$$a_2=C_0\cos\gamma-C_1V\cos\psi-C_2V\sin\psi \quad (50)$$

and ϕ in Eq. (49) is obtained from Eq. (48). At this point, from the equation for VP_V in system Eqs. (38), $dP_V/dt=-C_0/V<0$. The connection is from a B arc to a C arc.

However, if $P=0$ and boundary ϕ is used at the switching point, from Eq. (33) $\Omega=0$. From Eq. (36) the limiting value of n at this point is

$$n=\frac{\Delta E^*[(a_1V\sin\phi+a_2V\cos\phi)-P_\psi g\sin\phi\cos\gamma]}{\sin\gamma(C_0V+2P_\gamma g\cos\gamma)} \quad (51)$$

where a_1 and a_2 are given in Eqs. (50). At this point, from the equation for VP_V in system Eq. (38)

$$\frac{dP_V}{dt}=-\frac{1}{V}\left(C_0+\frac{2P_\gamma g\cos\gamma}{V}\right) \quad (52)$$

A switching from a C arc to a B arc is optimum if

$$C_0+2P_\gamma g\cos\gamma/V<0 \quad (53)$$

For a switching from a B arc to a C arc to be optimum, the preceding inequality is reversed. Along an S arc, we have $P_V=0$ and $dP_V/dt=0$ for a finite time interval. By taking the derivative of $dP_V/dt=0$, where dP_V/dt is given in Eq. (52), we have an equation for the linear thrust control

$$\frac{d^2P_V}{dt^2}=-\frac{C_0g}{V^2}\zeta\tau_{\max}+(\ldots)=0 \quad (54)$$

with $-C_0g/V^2\geq 0$ for optimal condition. However, this optimal condition is not satisfied with $C_0>0$. In the case where $P_\gamma=0$ at the switching point, from $\Omega=0$ it is obvious that $P_\psi=0$. From Eq. (51) the limiting value of n becomes

$$n=\frac{\Delta E^*}{C_0\sin\gamma}(a_1\sin\phi_{\max}+a_2\cos\phi_{\max}) \quad (55)$$

At this point, from Eq. (52), $dP_V/dt=-C_0/V<0$. The connection is from a B arc to a C arc.

Based on the preceding discussion of optimal switching, we can have some conclusions on the final arc of an optimal trajectory. According to the constraints on V_f, γ_f, and ψ_f, problems of flight in three dimensions can be classified into two cases, i.e., the case where V_f is free and the case where V_f is prescribed.

In the first case V_f is free; hence, $P_{V_f}=0$. Since $P_{V_f}=0$, the thrust control for the final arc is dictated by the derivative of the switching function P_V. The condition $dP_V/dt>0$ at the final time dictates a final C arc. If the inequality reverses, we have a final B arc, since at this point P_V is decreasing to the final value zero. In this case of free V_f there exist four different situations. First, γ_f and ψ_f are free; hence, $P_{\gamma_f}=P_{\psi_f}=0$. Since $P=0$ at the final point, for unbounded ϕ the limiting values of ϕ and n at the final point are given in Eqs. (48) and (49), respectively. For bounded ϕ, if $\phi_f=\phi_{\max}$, then the limiting value of n at the final point is given in Eq.

(55). Since $dP_V/dt = -C_0/V < 0$ at the final point, the final arc is always a B arc. Second, γ_f is free and ψ_f is prescribed; hence, $P_{\gamma f} = 0$ and $P_{\psi f} \neq 0$. Since $P \neq 0$ at the final point, n_f is always on the boundary. For unbounded bank angle, ϕ_f is nearly 90 deg, since from Eq. (25) $\tan\phi \to \infty$ at the final point, and $\phi_f = \phi_{\max}$ for bounded ϕ. For $n_f = n_s$, condition Eq. (42) with $P_{\gamma f} = 0$ at the final time dictates a final C arc. If this resulting inequality reverses, the final arc is a B arc. For $n_f = M_f^2 C_{L\max}/\omega_f$, condition Eq. (45) with $P_{\gamma f} = 0$ at the final time dictates a final C arc. If this resulting inequality reverses, the final arc is a B arc. Third, γ_f is prescribed and ψ_f is free; hence, $P_{\gamma f} \neq 0$ and $P_{\psi f} = 0$. Since $P \neq 0$ at the final point, n_f is always on the boundary and from Eq. (25) $\phi_f = 0$. For $n_f = n_s$, condition Eq. (42) with $P_{\psi f} = 0$ at the final time dictates a final C arc. If this resulting inequality reverses, the final arc is a B arc. For $n_f = M_f^2 C_{L\max}/\omega_f$, condition Eq. (45) with $P_{\psi f} = 0$ at the final time dictates a final C arc. If this resulting inequality reverses, the final arc is a B arc. Lastly, both γ_f and ψ_f are prescribed; hence $P_{\gamma f} \neq 0$ and $P_{\psi f} \neq 0$. Since $P \neq 0$ at the final time, n_f is always on the boundary and ϕ_f is given in Eq. (25). For $n_f = n_s$, condition Eq. (42) at the final time dictates a final C arc. If this resulting inequality reverses, the final arc is a B arc. For $n_f = M_f^2 C_{L\max}/\omega_f$, condition Eq. (45) at the final time dictates a final C arc. If this resulting inequality reverses, the final arc is a B arc.

In the second case V_f is prescribed; hence $P_{Vf} \neq 0$. In this case there also exist four different situations which are similar to those in the first case of free V_f. Hence, by similar procedures the optimal control of the last portion of the trajectory can be analyzed.

In the most general case, the solution requires the estimation of five parameters, i.e., C_1, C_2, C_3, P_{V0}, and $P_{\gamma 0}$. This, coupled with the optimal switching from one control regime to another, constitutes the main difficulty of the problem. The success in obtaining the solution depends on the knowledge of the particular flight program considered.

Numerical Examples

Minimum-Time Three-Dimensional Turn to a Heading

In this problem the initial conditions are

$$t=0,\ X=0, Y=0,\ Z=Z_0,\ V=V_0,\ \gamma=\gamma_0,\ \psi=0\,\text{deg} \qquad (56)$$

and the final conditions are

$$t_f=\min,\ X_f=\text{free},\ Y_f=\text{free},\ Z=Z_f,$$
$$V_f=\text{free},\ \gamma_f=\text{free},\ \psi=\psi_f \qquad (57)$$

Hence, the transversality conditions are

$$C_1=0,\ C_2=0,\ P_{Vf}=0,\ P_{\gamma f}=0 \qquad (58)$$

Since $C_1 = 0$ and $C_2 = 0$, the number of parameters is reduced from five to three. Therefore, the problem in terms of C_3, P_{V0}, and $P_{\gamma 0}$ is a three-parameter problem. These three parameters are to be selected to satisfy the final conditions Eq. (57) and the transversality conditions Eq. (58). For this numerical example we choose $\psi_f = 180$-deg and $Z_f > Z_0$, i.e., the problem of minimum-time supersonic chandelle, which is a three-dimensional 180-deg climbing turn. Since we are interested in generating a family of optimal trajectories of minimum-time supersonic chandelle starting from the offset point,† referred to as the initial point, to the different final altitudes depending on the arrival at the attack cone, we can use one parameter as a scanning parameter. Hence the problem becomes a two-parameter problem. For the solution we select C_3 as a scanning parameter, and for each C_3 we guess P_{V0} and $P_{\gamma 0}$ and start the integration of the state Eqs. (1) and the adjoint Eqs. (38) and (39) using the optimal thrust and aerodynamic control law. At $\psi_f = 180$ deg, the conditions $P_{Vf} = 0$ and $P_{\gamma f} = 0$ are used to adjust the two unknown parameters P_{V0} and $P_{\gamma 0}$. This results in a Z_f. Figure 5 shows the results of a family of trajectories 1-5 obtained by running a very high-speed digital computer in real-time, on-line using the data of the supersonic fighter model. In this problem, the minimum-time supersonic chandelle is designed to complete a course reversal climbing from $Z_0 = 8$ km to a higher altitude which lies somewhere between $Z_f = 18$ km of trajectory 1 and $Z_f = 19.5$ km of trajectory 5. This altitude gain is now function of C_3. Note that higher altitude gain corresponds to higher C_3, and for each C_3 a final altitude can be obtained. On the other hand, the Mach number decreases from an initial Mach two to a lower M_f which is between 1.21 of trajectory 5 and 1.35 of trajectory 1. Thus, for higher Z_f the M_f is lower. The final altitude of trajectories 1, 2, 3, 4, and 5 are, respectively, 18, 18.4, 18.7, 19, and 19.5 km; and their final Mach numbers are, respectively, 1.35, 131, 1.28, 1.26 and 1.21.

The constraints $\phi_{\max} = 1.5$ rad and $n_s = 4.5$ are imposed on all the five trajectories. The difficulty in evaluating P_{Z0} when $\gamma_0 = 0$ is avoided by using initially a slightly positive value of γ_0 since the trajectory has the tendency to start with a climb for a high initial Mach two. As predicted, the last portion of each of the five trajectories is flown with boundary ϕ and boundary n. Since $n_f = M^2 C_{L\max}/\omega_f$ is used at the final point, condition Eq. (45) with $P_{\gamma f} = 0$ is not satisfied for any of the five trajectories at the final time for the given function $C_{L\max}(M)$. Hence, as predicted, the final arc is a B arc for all five trajectories.

Minimum-Time Three-Dimensional Turn to a Point

In this problem, the initial conditions are the same as those in the previous problem of turn to a heading, but the final conditions are now

$$t_f=\min,\ X=X_f,\ Y=Y_f,\ Z=Z_f,\ V_f=\text{free},\ \gamma_f=\text{free},\ \psi=\psi_f \qquad (59)$$

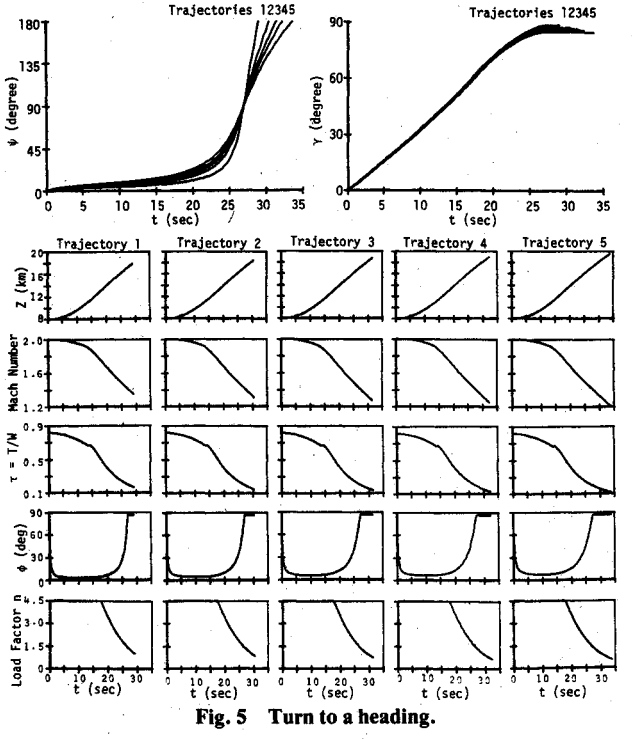

Fig. 5 Turn to a heading.

†Offset point is defined here as the position when the supersonic fighter arrives at Mach two and is ready to immediately initiate the minimum-time supersonic chandelle to reach the attack cone. The attack cone is any position to the rear of the target from which we can maneuver and overtake the target into the position of the weapon firing ranges.

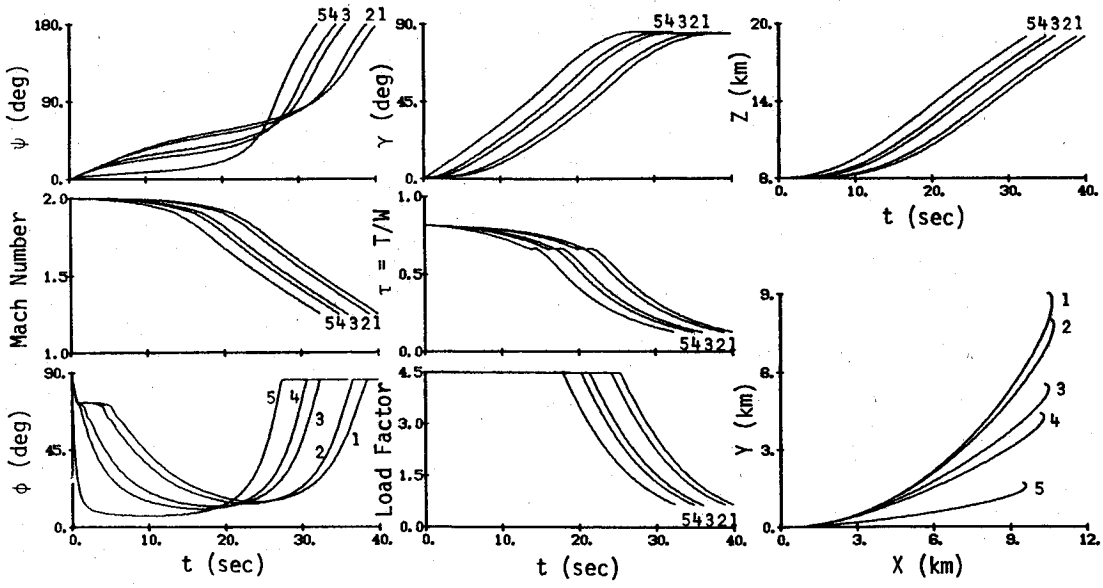

Fig. 6 Turn to a point.

Hence, the transversality conditions are now

$$P_{V_f}=0, \qquad P_{\gamma_f}=0 \tag{60}$$

Since X_f and Y_f are now prescribed, we have $C_1 \neq 0$ and $C_2 \neq 0$. The problem in terms of C_1, C_2, C_3, P_{V0}, and $P_{\gamma 0}$ is a five-parameter problem. These five parameters are to be selected to satisfy the final conditions Eq. (59) and the transversality conditions Eq. (60). To obtain the solution we guess C_1, C_2, C_3, P_{V0}, and $P_{\gamma 0}$ and start the integration of the state Eqs. (1) and the adjoint Eqs. (38) and (39) using optimal thrust and aerodynamic control law. At $\psi=\psi_f$ the conditions on $X=X_f$, $Y=Y_f$, $Z=Z_f$, $P_{V_f}=0$, and $P_{\gamma_f}=0$ are used to adjust the five unknown parameters. Figure 6 gives a comparison of five trajectories whose initial conditions are the same as those in Fig. 5. As in the previous example, all five trajectories in this figure are generated in real-time, on-line. They all have the same $h_f=19$ km and the same $\psi_f=180$ deg but different prescribed X_f and different prescribed Y_f. For trajectory 1, $X_f=10.5$ km and $Y_f=9$ km; for trajectory 2, $X_f=10.5$ km and $Y_f=8$ km; for trajectory 3, $X_f=10.4$ km and $Y_f=5.5$ km; for trajectory 4, $X_f=10.2$ km and $Y_f=4.4$ km; and for trajectory 5, both X_f and Y_f are free. For comparison to the maneuver of turn to a heading in the previous example, trajectory 5 in this figure is a duplicate of trajectory 4 in Fig. 5. The final time for trajectories 1, 2, 3, 4, and 5 in Fig. 6 are, respectively, 40.1, 38.8, 36, 34.8, and 32.3 sec. Comparing trajectory 5 with the other four trajectories it is seen that for the same prescribed $Z_f=19$ km and the same prescribed $\psi_f=180$ deg, trajectory 5 with free X_f and free Y_f has the shortest final time. As seen in Fig. 6, for the same prescribed $X_f=10.5$ km, trajectory 1 has a longer prescribed Y_f than trajectory 2 and, therefore, takes longer time to complete. In general, for the same prescribed Z_f and $\psi_f=180$ deg, three-dimensional turns with larger X_f and Y_f require longer time to complete.

As in the previous numerical example, the constraints $\phi_{\max}=1.5$ rad and $n_s=4.5$ are imposed on all the five trajectories in this problem. Again, the difficulty in evaluating the initial value of P_Z when $\gamma_0=0$ is avoided by using initially a slightly positive value of γ_0 since the trajectory has the tendency to start with a climb for a high initial Mach two. As predicted, the last portion of each of the five trajectories is flown with boundary ϕ and boundary n. Since $n_f=M^2C_{L_{\max}}/\omega_f$ is used at the final point, condition Eq. (45) with $P_{\gamma_f}=0$ is not satisfied for any of the five trajectories at the final time for the given function $C_{L_{\max}}(M)$. Hence, as predicted, the final arc is a B arc for all five trajectories.

In the case where ψ_f is free, we have

$$P_{\psi_f}=C_1Y_f-C_2X_f+C_3=0 \tag{61}$$

Using this condition we have

$$P_\psi=C_1(Y-Y_f)-C_2(X-X_f) \tag{62}$$

Therefore, it is obvious that in this case of free ψ_f the number of parameters is reduced from five to four. The problem in terms of C_1, C_2, P_{V0}, and $P_{\gamma 0}$ is a four-parameter problem. To obtain the solution, we guess these four parameters and start the integration of the state Eqs. (1) and the adjoint equations using the optimal thrust and aerodynamic control law. At Z_f the conditions on $P_{V_f}=0$, $P_{\gamma_f}=0$, $P_{\psi_f}=0$, and $X=X_f$ are used to adjust these four unknown parameters. As mentioned previously, since $P_{V_f}=0$, $P_{\gamma_f}=0$, and $P_{\psi_f}=0$ the final arc is always a B arc. For unbounded ϕ, the limiting values of ϕ and n at the final point are given in Eqs. (48) and (49), respectively. For bounded ϕ, if $\phi_f=\phi_{\max}$, then the limiting value of n at the final point is given in Eq. (55).

Conclusion

On the whole, this paper presents clearer insight into the thrust and aerodynamic controls in supersonic aircraft maneuvers as compared to what has been done in the past. The proposed method of solution is efficient and presents no ambiguity on the selection of the optimal thrust-to-weight ratio, the bank angle, and the angle-of-attack (lift coefficient or load factor) controls. The technique should be useful for performance assessment of supersonic aircraft with potential for implementation of onboard flight control system.

References

[1] Lin, C.F., "Optimum Maneuvers of Supersonic Aircraft," Ph.D. Dissertation, Vols. 1 and 2, The University of Michigan, 1980.

[2] Bryson, A.E. Jr. and Parsons, M.G., "Constant-Altitude, Minimum-Time Turns to a Line and to a Point for a Supersonic Aircraft with a Constraint on Maximum Velocity," Stanford University, Stanford, Calif., SUDAAR 437, Nov. 1971.

[3]Erzberger, H. and Lee, H.Q., "Optimum Horizontal Guidance Techniques for Aircraft," *Journal of Aircraft,* Vol. 8, Feb. 1971, pp. 95-101.

[4]Hedrick, J.K. and Bryson, A.E., "Minimum Time Turns for a Supersonic Airplane at Constant Altitude," *Journal of Aircraft,* Vol. 8, March 1971, pp. 182-187.

[5]Uehara, S., Stewart, H.J., and Wood, L.J., "Minimum Time Loop Maneuvers of Jet Aircraft," *Journal of Aircraft,* Vol. 15, Aug. 1978, pp. 449-455.

[6]Shinar, J., Yair, D., and Rotman, Y., "Analysis of Optimal Loop and Split-S by Energy State Modeling," *Israel Journal of Technology,* Vol. 16, 1978, pp. 70-82.

[7]Bryson, A.E. Jr. and Denham, W., "A Steepest Ascent Method for Solving Optimum Programming Problems," *Journal of Applied Mechanics,* Vol. 29, June 1962, pp. 247-257.

[8]Breakwell, J.V., "Optimal Flight Path Angle Transitions in Minimum-Time Airplane Climbs," *Journal of Aircraft,* Vol. 14, Aug. 1977, pp. 782-786.

[9]Kelley, H.J., Falco, M., and Ball, D.J., "Air Vehicle Trajectory Optimization," SIAM Symposium on Multivariable System Theory, Cambridge, Mass., Nov. 1-3, 1962.

[10]Kelley, H.J., "Aircraft Maneuver Optimization by Reduced Order Approximation," *Control and Dynamic Systems,* edited by C.T. Leondes, Academic Press, New York, 1973.

[11]Hedrick, J.K. and Bryson, A.E. Jr., "Three-Dimensional, Minimum-Time Turns for a Supersonic Aircraft," *Journal of Aircraft,* Vol. 9, Feb. 1972, pp. 115-121.

[12]Parsons, M.G., Bryson, A.E., and Hoffman, W.C., "Long-Range Energy-State Maneuvers for Minimum Time to Specified Terminal Conditions," *Journal of Optimization Theory and Applications,* Vol. 17, 1975, pp. 447-463.

[13]Vinh, N.X., "Optimal Singular Control with Applications to Trajectory Optimization," NASA CR-3087, 1979.